Mon. Not. R. Astron. Soc. **000**, 1–11 (2002) Printed 8 April 2013 (MN LATEX style file v2.2)

arXiv:1304.1550v1 [astro-ph.GA] 4 Apr 2013

The moment of core collapse in star clusters with a mass function

M. S. Fujii[1] ⋆ and S. Portegies Zwart[1]⋆
[1] *Leiden Observatory, Leiden University, NL-2300RA Leiden, The Netherlands*

Accepted 1988 December 15. Received 1988 December 14; in original form 1988 October 11

ABSTRACT

Star clusters with multi-mass components dynamically evolve faster than those modelled with equal-mass components. Using a series of direct N-body simulations, we investigate the dynamical evolution of star clusters with mass functions, especially their core collapse time. Multi-mass clusters tend to behave like systems with a smaller number of particles, which we call the effective number of particles ($N_{\rm eff}$) and for which $N_{\rm eff} = M/m_{\rm max}$ (here M and $m_{\rm max}$ are the total cluster mass and the mass of the most massive star in the cluster, respectively). We find that the time of core collapse is inversely proportional to the mass of the most massive star in the cluster and analytically confirm that this is because the core collapse of clusters with a mass function proceeds on the dynamical friction timescale of the most massive stars. As the mass of the most massive star increases, however, the core-collapse time, which is observed as a core bounce of the cluster core from the evolution of the core density or core radius, becomes ambiguous. We find that in that case the total binding energy of the hard binaries gives a good diagnosis for determining the moment at which the cluster core collapses. Based on the results of our simulations, we argue that the core bounce becomes ambiguous when the mass of the most massive star exceeds 0.1% of the total mass of the cluster.

Key words: galaxies: star clusters: general — methods: numerical

1 INTRODUCTION

Star clusters are collisional systems with a negative heat capacity, and therefore they dynamically evolve to eventually reach core collapse. The process to core collapse is simply described using a semi-analytic treatment of the energy transfer from the cluster core to the outer part of the cluster (Lynden-Bell & Wood 1968), and it was confirmed using various methods such as gaseous models (Nakada 1978; Bettwieser & Sugimoto 1984), Fokker-Planck simulations (Inagaki 1980; Cohn 1980; Lynden-Bell & Eggleton 1980), and direct N-body simulations (Bettwieser & Sugimoto 1985; Makino et al. 1986). Because of the high stellar density of the core during its collapse, dynamical binaries form in this phase (Spitzer & Hart 1971; Aarseth 1974). Once binaries form in the core, they generate energy which is transported outward by interactions with other cluster members (Heggie 1975; Hut 1983). Due to the binary heating the core finally bounces, and then the core oscillates when the number of stars is sufficiently large (Sugimoto & Bettwieser 1983). Such gravothermal oscillation was first found using gaseous models (Sugimoto & Bettwieser 1983; Bettwieser & Sugimoto 1984) but the behaviour was later confirmed using direct N-body (Makino et al. 1986; Makino 1996) and Fokker-Planck (Goodman 1987) simulations.

The time between cluster birth and the moment of core collapse (what we will call the core-collapse time, or $t_{\rm cc}$) is proportional to the two-body relaxation time at the half-mass radius $t_{\rm rh}$ (Spitzer 1987). For clusters in which all stars have the same mass, the core collapses at $t_{\rm cc} \simeq 15 t_{\rm rh}$. This result has a theoretical background and was confirmed with simulations using a wide variety of techniques: Monte-Carlo methods (Spitzer & Shull 1975), Fokker-Planck calculations (Cohn 1979), and direct N-body simulations (Makino 1996). With a spectrum of stellar masses, however, the core-collapse time becomes much shorter than when all stars have the same mass (Inagaki & Wiyanto 1984). From direct N-body simulations, it is obtained that $t_{\rm cc} \simeq 0.2 t_{\rm rh}$ with a realistic mass function (Portegies Zwart & McMillan 2002).

Gürkan et al. (2004) performed a large number of Monte Carlo simulations covering a wide range of the concentration parameters and mass functions. They showed that the core-collapse time scales with the central relaxation time, $t_{\rm rc}$ rather than with $t_{\rm rh}$. Here the central relaxation

---

⋆ E-mail: fujii@strw.leidenuniv.nl(MSF); spz@strw.leidenuniv.nl(SPZ)

© 2002 RAS

time is defined as

$$t_{\rm rc} \equiv \frac{0.065\sigma_{\rm c,3D}^3}{G^2\langle m\rangle \rho_{\rm c} \ln \Lambda}, \quad (1)$$

where $\sigma_{\rm c,3D}$ and $\rho_{\rm c}$ are the central three-dimensional velocity dispersion and core density, respectively (Spitzer 1987; Gürkan et al. 2004). The Coulomb logarithm, $\ln\Lambda$, is written as $\ln\gamma N$, where N is the total number of stars. For the central relaxation time of star clusters, it is numerically obtained that $\gamma = 0.015$ (Giersz & Heggie 1996) (the classic theoretical value for $t_{\rm rh}$ with single-mass components is $\gamma = 0.11$ Spitzer (1987)).

In the case with a power-law mass function in which $m_{\rm max}$ and $\langle m\rangle$ are the maximum mass and the mean mass of the stellar mass distribution, Gürkan et al. (2004) found that the core-collapse time $t_{\rm cc} \propto (m_{\rm max}/\langle m\rangle)^{-1.3}$. They also demonstrated the existence of a minimum to the core-collapse time, which is $t_{\rm cc}/t_{\rm rc} = 0.15$. This value is also seen in Goswami et al. (2012), in which they use the same Monte Carlo code that was adopted by Gürkan et al. (2004), but with a wider range of initial conditions including initially mass-segregated models. The arguments for the particular exponent (being -1.3) and the minimum to the core-collapse time, however, was not discussed and remains unclear.

In this paper we show the results of core collapse simulations of star clusters with power-law mass functions using direct N-body simulations. We find that the core collapse time scales $t_{\rm cc} \propto (m_{\rm max}/\langle m\rangle)^{-1}$, contrary to the earlier finding of Gürkan et al. (2004), but we support our finding with analytic arguments. We further argue that core collapse is driven by the sinking of the most massive star to the cluster centre, by dynamical friction (as was suggested in Portegies Zwart & McMillan (2002)). The minimum to the core-collapse time then corresponds to the time required for the most massive star to reach the cluster centre. For the most extreme mass functions the minimum core-collapse time then naturally depends on the crossing time of the system. The core bounce becomes less pronounced for larger values of $m_{\rm max}/\langle m\rangle$, and this is qualitatively understood from the dynamical evolution being driven by the most massive stars in the cluster. For a mass ratio $M/m_{\rm max} \lesssim 10^3$ core collapse becomes hard to determine, and it even becomes indistinguishable for $M/m_{\rm max} \lesssim 100$, because in those cases the core will eventually be composed of only a few massive stars, almost irrespective of the total number of stars in the cluster.

2 N-BODY SIMULATIONS AND THE INITIAL CONDITIONS

We performed a series of N-body simulations using King models (King 1966) with a non-dimensional concentration parameter, W_0, of 3 and 6 as initial density profiles. Hereafter, we adopt N-body units in which, $G = M = -4E = 1$, where G, M, and E are the gravitational constant, the total mass, and the total energy of the cluster, respectively (Heggie 1975)[1]. In table 1 we summarize the initial conditions for the runs. For each simulation we adopted N particles from $N = 2048$ (2k), 8192 (8k), 32768 (32k) to $N = 1310172$ (128k), with a power-law mass function with exponent α and an upper-mass limit of $m_{\rm max}$. The value of $m_{\rm max}/\langle m\rangle$ is varied from 1.0 (equal mass) to 517, but for models with fewer particles we adopted a smaller value of $m_{\rm max}$. For the mass function exponent α, we adopted $\alpha = 2.35$ (Salpeter 1955), 1.7, and 1.2. In Tables 2 and 3 we summarize the simulation results.

All simulations are performed using the sixth-order predictor-corrector Hermite scheme (Nitadori & Makino 2008) running on GPU using the Sapporo2 library (Belleman et al. 2008; Bédorf & Portegies Zwart 2012) and also on CPU clusters using the two-dimensional parallelization scheme by Nitadori et al. (2006). We used a time step criterion (Nitadori & Makino 2008) with accuracy parameter, η =0.1–0.3. The energy error $\lesssim 10^{-5}$ for all simulations over the entire duration of the simulation. In some cases the time step of the calculations dropped below $\sim 10^{-13}$, which occurs near the moment of the formation of a binary of a few $100kT$ for the models and with $m_{\rm max}/\langle m\rangle \lesssim 2$. (We express binding energies in terms of $kT \equiv \langle m\rangle\sigma_{\rm 1D}^2$, where $\sigma_{\rm 1D}$ is the one-dimensional velocity dispersion of the cluster, $3NkT/2$ is the initial kinetic energy of the entire system.) To prevent even smaller time steps, which have unpleasant consequences for the performance, we adopted a small softening ϵ; for the simulations with $W_0 = 3$ we adopted $\epsilon = 1/(200N)$ and $\epsilon = 1/(130N)$ for models with $W_0 = 6$. With this softening we are able to resolve binaries with a semi-major axis of a $1200kT$ and $780kT$ for the simulations with $W_0 = 3$ and $W_0 = 6$, respectively.

3 CORE COLLAPSE IN MULTI-MASS CLUSTERS

The core-collapse time is determined by the moment of core bounce, which is seen in the time evolution of the core radius or core density. For some models it is difficult to distinguish the core collapse, because there does not seem to be a peak in the density evolution or a depression in the core radius. Another indicator for determining the moment of core collapse is by monitoring the evolution of the binding energy of dynamically formed binaries. During the core collapse, hard binaries form in the cluster. They are hardened by three-body encounters in the cluster core and generate the energy for the core bounce. In this section, we present the evolution of the core radius and the density from the simulations, and then we discuss the relation between the core evolution and the dynamically formed binaries in order to provide an objective determination of the moment of core collapse and ultimately define the core collapse.

3.1 The evolution of core density and radius

In Figure 1 we present the evolution of the core density and the core radius for an equal-mass model with $W_0 = 3$, N =2k (left) and the same model but with a Salpeter mass function with $m_{\rm max}/\langle m\rangle = 8$ (right). We calculate the core radius and density using a method of Casertano & Hut (1985), but we took into account the mass of the central particles. Compared to the equal mass case, the core collapse in the models with $m_{\rm max}/\langle m\rangle \gtrsim 8$ is less clear, although the core noticeably expands after a slight depression.

---

[1] see also `http://en.wikipedia.org/wiki/N-body_units`.

Table 1. Properties of King Models

W_0	$\rho_{\rm c}$	$\sigma_{\rm c,1D}$	$\sigma_{\rm 1D}$	$r_{\rm c}$	$r_{\rm h}$	$M_{\rm c}$
3	0.652	0.518	0.520	0.543	0.839	0.238
6	2.11	0.503	0.636	0.293	0.804	0.117

If we increase $m_{\rm max}/\langle m\rangle$, the core collapse becomes more ambiguous. In Figure 2 we present the results of the same simulation as we presented in Figure 1, but with $m_{\rm max}/\langle m\rangle = 32$ (left in Fig. 2) and 129 (right). In these simulations the mass of the most massive star is comparable to the mass of the initial cluster core. After the core shrinks, it keeps the small core radius and slowly expands (see right panel of Figure 2).

Based on our simulations we conclude that a core bounce occurs if $M/m_{\rm max} \gtrsim 10^3$, and the rapid core expansion becomes apparent only if $M/m_{\rm max} \gtrsim 100$. We illustrate these in the left panel of Figure 3, where we present the same models as in Figure 2 but with $N = 128$k. This model satisfies the first criterion ($M/m_{\rm max} \gtrsim 10^3$) and as expected the core bounce is clearly visible. With $m_{\rm max}/\langle m\rangle = 517$ (the right panel of Figure 3), however, which does not satisfy either of the criteria and as a consequence the core bounce is obscured. These criteria are similar to the Spitzer instability (Spitzer 1987). In the case of multi-mass components, the criterion for the Spitzer instability is $M/m_{\rm max} \sim 10^4$ (Breen & Heggie 2012a). We discuss these criteria further in section 4.

3.2 The determination of core-collapse time using hard binaries

In the previous subsection we discussed the lack of a core bounce for the case where $M/m_{\rm max} \lesssim 10^3$. In particular if $M/m_{\rm max} \lesssim 100$, the core in these cases however still expands quite dramatically after some time. In these cases it becomes very hard to use the core size or density peak to determine the moment of core collapse, but the expansion of the core indicates that something like a core collapse must have happened. In order to quantify this moment we focus on the evolution of hard (dynamically formed) binaries, which are suspected to generate the energy that causes the core to bounce.

In the bottom panels in Figures 1, 2, and 3, we present the total binding energy of hard binaries in the various simulations. We accumulated the binding energy of hard binaries (with $> 3kT$), but the total binding energy is almost comparable to that of the hardest binary. By comparison of the evolution of the binding energy with the core density (or core radius), we observe that the moment of the core bounce is consistently occurring at the same moment that the total binding energy in hard binaries reaches a few hundreds of kT.

We estimate the critical binding energy for the core bounce from a discussion on the energy emitted by the hard binary via a three-body encounter. In the dynamical evolution of star clusters through core collapse, the cluster responds to a core collapse by a bounce, and the occurrence is associated with the moment when the energy produced by hard binaries exceeds the potential energy of the cluster core ϕ_0 (Hut 1996; Heggie & Hut 2003). The energy released in an encounter between a single star and a binary with binding energy $E_{\rm bin}$ is $\Delta E_{\rm bin} = 0.4E_{\rm bin}$ (Heggie 1975). The core then bounces when the binding energy of the hard binary satisfies

$$E_{\rm bin} > \frac{1}{0.4}\langle m\rangle\phi_0. \tag{2}$$

Following the discussion in Hut (1996), assuming that the core is virialized at the moment of the bounce, the potential energy of the core is $\phi_0 = 2K = N_{\rm c}\langle m\rangle\sigma^2_{\rm c,3D}$. Here we adopt $\sigma_{\rm c,3D}$ for the velocity dispersion of the stars in the core and K is the kinetic energy of the core. In order to be able to bounce the core, the binaries should have a binding energy of at least

$$\begin{aligned} E_{\rm bin,cr} &\sim \frac{1}{0.4}N_{\rm c}\langle m\rangle\sigma^2_{\rm c,3D} & (3)\\ &\sim 200\langle m\rangle\sigma^2_{\rm c,3D}. & (4)\end{aligned}$$

Here we adopted $N_{\rm c} \sim 80$ (Hut 1996). Although $\sigma_{\rm c,3D}$ is the velocity dispersion at the moment of core bounce, we assume that it is similar to the initial core velocity dispersion, $\sigma_{\rm c,0,3D}$, because the core evolves following $\rho_{\rm c} \propto r^{-\kappa}$ and $\kappa = 2.2$–2.3 during the core collapse (Cohn 1980; Lynden-Bell & Eggleton 1980; Takahashi 1995; Heggie & Hut 2003), and therefore the velocity dispersion changes only by a factor of 2 (Giersz & Heggie 1996). From the definition of kT, the critical binding energy for core bounce is obtained as $E_{\rm bin,cr} \sim (200\sigma^2_{c,0,3D}/\sigma^2_{\rm 1D})kT = (600\sigma^2_{c,0,1D}/\sigma^2_{\rm 1D})kT$. In the case of King models with $W_0 = 3$ and 6, $E_{\rm bin,cr} \sim 600kT$ and $390kT$, respectively. This estimate is consistent with the peak in the binding energy distribution of escaping binaries obtained from a direct N-body simulations in equal-mass simulations (see Figure 22 in Tanikawa & Fukushige 2009). In Figure 4, we present the relation between the core-collapse time obtained from the evolution of core density (or radius) and that obtained from the earlier discussed requirement $E_{\rm bin} > E_{\rm bin,cr}$. Both appear to predict consistently the same moment for the core collapse, and we can adopt the binary binding energy argument to obtain an objective and physically motivated argument for the moment of core bounces, and therefore for the moment of core collapse. Hereafter we adopt this criterion to define the moment of core collapse.

3.3 The core-collapse time

In Figure 5 we present $t_{\rm cc}/t_{\rm rc}$ as a function of $m_{\rm max}/\langle m\rangle$. Here we defined the core-collapse time $t_{\rm cc}$ as the moment when the total biding energy of hard binaries in the cluster exceeds $600kT$ and $390kT$ for models with $W_0 = 3$ and $W_0 = 6$, respectively. The core-collapse time for single-mass component models is $t_{\rm cc}/t_{\rm rc} \simeq 20$ for $W_0 = 3$ and

Table 2. Models with $W_0 = 3$

Model	W_0	α	$m_{\rm min}/\langle m\rangle$	$m_{\rm max}/\langle m\rangle$	N	ϵ	$t_{\rm cc}$	$t_{\rm 600kT}$
w3-2k-eq	3	-	1.0	1.0	2k	$1/(200N)$	735	750
w3-8k-eq	3	-	1.0	1.0	8k	$1/(200N)$	2.41×10^3	2.41×10^3
w3-2k-m2-Sal	3	2.35	0.607	2.02	2k	$1/(200N)$	435	442
w3-8k-m2-Sal	3	2.35	0.607	2.02	8k	$1/(200N)$	1.26×10^3	1.26×10^3
w3-2k-m8-Sal	3	2.35	0.391	8.07	2k	0	85	92
w3-8k-m8-Sal	3	2.35	0.391	8.07	8k	0	297	300
w3-2k-m32-Sal	3	2.35	0.329	32.3	2k	0	33	39.5
w3-8k-m32-Sal	3	2.35	0.329	32.3	8k	0	55	61.2
w3-32k-m32-Sal	3	2.35	0.329	32.3	32k	0	217	225
w3-2k-m129-Sal-1	3	2.35	0.296	129.2	2k	0	13	12.6
w3-2k-m129-Sal-2	3	2.35	0.296	129.2	2k	0	19	22.1
w3-8k-m129-Sal	3	2.35	0.296	129.2	8k	0	35	29.4
w3-32k-m129-Sal	3	2.35	0.296	129.2	32k	0	74.6	81.9
w3-128k-m129-Sal	3	2.35	0.279	516.6	128k	0	175	172
w3-2k-m258-Sal-1	3	2.35	0.286	258.3	2k	0	-	15.6
w3-2k-m258-Sal-2	3	2.35	0.286	258.3	2k	0	-	19.3
w3-8k-m258-Sal	3	2.35	0.286	258.3	8k	0	22.8	21.1
w3-32k-m258-Sal	3	2.35	0.286	258.3	32k	0	62	64.0
w3-2k-m517-Sal-1	3	2.35	0.279	516.6	2k	0	-	15.6
w3-2k-m517-Sal-2	3	2.35	0.279	516.6	2k	0	-	22.9
w3-8k-m517-Sal	3	2.35	0.279	516.6	8k	0	-	23.9
w3-32k-m517-Sal	3	2.35	0.279	516.6	32k	0	30.0	30.1
w3-128k-m517-Sal	3	2.35	0.279	516.6	128k	0	40.7	36.3
w3-2k-m2-a1.2	3	1.2	0.442	2.02	2k	$1/(200N)$	341	346
w3-8k-m2-a1.2	3	1.2	0.442	2.02	8k	$1/(200N)$	1.19×10^3	1.14×10^3
w3-2k-m8-a1.2	3	1.2	0.0336	8.07	2k	0	88	127
w3-8k-m8-a1.2	3	1.2	0.0336	8.07	8k	0	294	294
w3-2k-m32-a1.2	3	1.2	5.28×10^{-4}	32.3	2k	0	32	39.3
w3-8k-m32-a1.2	3	1.2	5.28×10^{-4}	32.3	8k	0	99	96.8
w3-2k-m129-a1.2	3	1.2	5.16×10^{-6}	129.2	2k	0	-	18
w3-8k-m129-a1.2	3	1.2	5.16×10^{-6}	129.2	8k	0	-	26.5
w3-32k-m129-a1.2	3	1.2	5.16×10^{-6}	129.2	32k	0	92.8	98.6
w3-2k-m258-a1.2	3	1.2	2.13×10^{-8}	258.3	2k	0	-	17.8
w3-8k-m258-a1.2	3	1.2	2.13×10^{-8}	258.3	8k	0	-	16.4
w3-8k-m517-a1.2	3	1.2	1.23×10^{-8}	516.6	8k	0	9.7	8.94
w3-32k-m517-a1.2	3	1.2	1.23×10^{-8}	516.6	32k	0	-	46.1
w3-2k-m2-a1.7	3	1.7	0.525	2.02	2k	$1/(200N)$	414	426
w3-2k-m8-a1.7	3	1.7	0.192	8.07	2k	0	98	108
w3-2k-m32-a1.7	3	1.7	0.0856	32.3	2k	0	36	37.6
w3-8k-m32-a1.7	3	1.7	0.0856	32.3	8k	0	70.5	73.3
w3-2k-m129-a1.7	3	1.7	0.0403	129.2	2k	0	11	10.8
w3-8k-m258-a1.7	3	1.7	0.0304	258.3	8k	0	-	11.6

$t_{\rm cc}$ is the core-collapse time obtained from the core density evolution, while $t_{\rm 600kT}$ is the time in which the total binding energy of hard binaries in the cluster exceed $600kT$. Here we defined $t_{\rm 600kT}$ (for models with $W_0 = 3$) and $t_{\rm 390kT}$ (for models with $W_0 = 6$) as the time when, for the first time, $E_{\rm bin} > E_{\rm bin,cr}$.

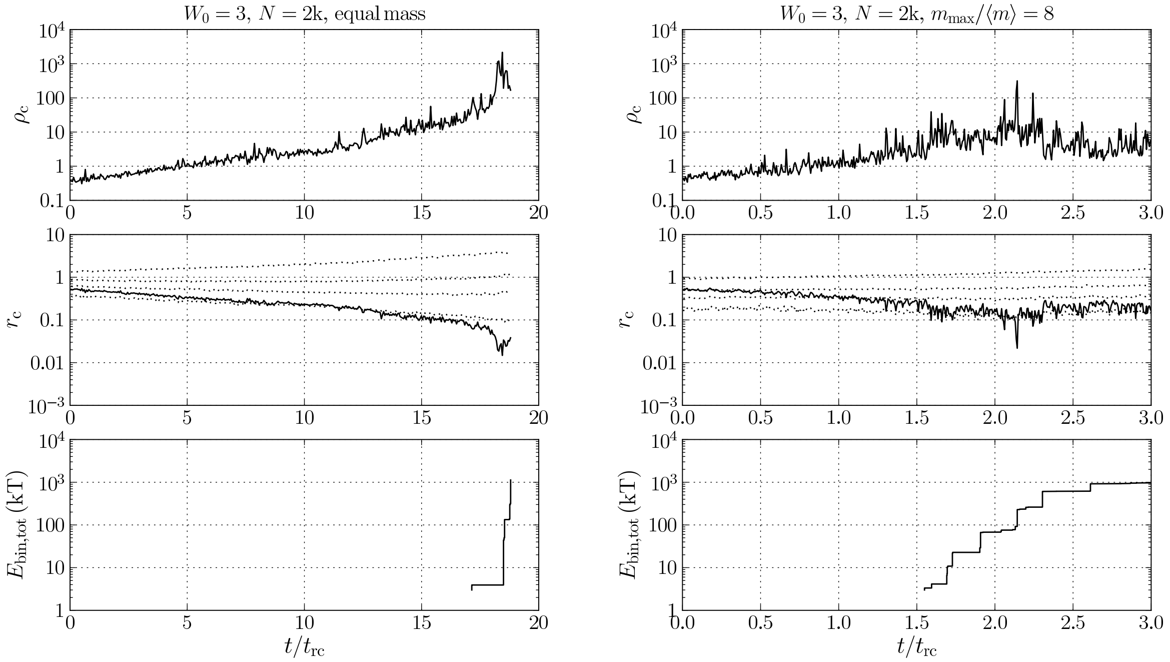

Figure 1. Time evolution of the cluster parameters. To panel: the evolution of the core density. Middle panel: evolution of the core radius (solid) and the 10%, 30, 50 and 80% (bottom to top) Lagrangian radii (dotted curves). Bottom panel: the total binding energy in hard binaries. The left three panels give the results for the model with $W_0 = 3$ for equal mass stars, and the right three panels give the results for a mass function with $\alpha = 2.35$ and $m_{\rm max}/(\langle m\rangle = 8$.

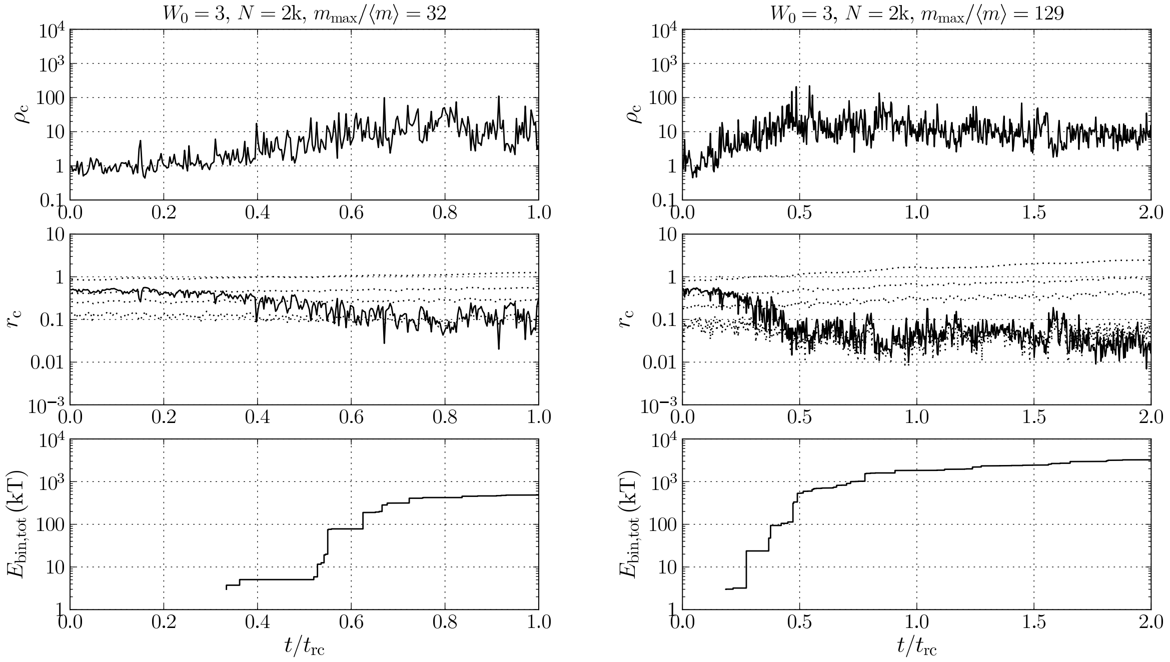

Figure 2. Same as Figure 1, but for models with $m_{\rm max}/(\langle m\rangle = 32$ (left) and 129 (right).

Table 3. Models with $W_0 = 6$

Model	W_0	α	$m_{\rm min}/\langle m\rangle$	$m_{\rm max}/\langle m\rangle$	N	ϵ	$t_{\rm cc}$	$t_{\rm 390kT}$
w6-2k-eq	6	-	1.0	1.0	2k	$1/(130N)$	650	652
w6-8k-eq	6	-	1.0	1.0	8k	$1/(130N)$	1.86×10^3	1.86×10^3
w6-2k-m2-Sal	6	2.35	0.607	2.02	2k	$1/(130N)$	230	251
w6-8k-m2-Sal	6	2.35	0.607	2.02	8k	$1/(130N)$	806	808
w6-2k-m8-Sal	6	2.35	0.391	8.07	2k	0	51.8	52.9
w6-8k-m8-Sal	6	2.35	0.391	8.07	8k	0	114	138
w6-2k-m32-Sal	6	2.35	0.329	32.3	2k	0	19.9	13.1
w6-8k-m32-Sal	6	2.35	0.329	32.3	8k	0	31.9	31.9
w6-2k-m129-Sal	6	2.35	0.296	129.2	2k	0	15.5	17.3
w6-8k-m129-Sal	6	2.35	0.296	129.2	8k	0	18.6	15.4
w6-32k-m129-Sal	6	2.35	0.296	129.2	32k	0	34	35.1
w6-2k-m517-Sal	6	2.35	0.279	516.6	2k	0	-	38.0
w6-8k-m517-Sal	6	2.35	0.279	516.6	8k	0	-	10.1
w6-32k-m517-Sal	6	2.35	0.279	516.6	32k	0	16.8	14.6
w6-2k-m2-a1.2	6	1.2	0.442	2.02	2k	0	240	267
w6-8k-m2-a1.2	6	1.2	0.442	2.02	8k	0	825	819
w6-2k-m8-a1.2	6	1.2	0.0336	8.07	2k	0	49	50.3
w6-8k-m8-a1.2	6	1.2	0.0336	8.07	8k	0	170	196
w6-2k-m32-a1.2	6	1.2	5.28×10^{-4}	32.3	2k	0	-	24.9
w6-8k-m32-a1.2	6	1.2	5.28×10^{-4}	32.3	8k	0	60	55.9
w6-2k-m129-a1.2	6	1.2	5.16×10^{-6}	129.2	2k	0	-	12.8
w6-8k-m129-a1.2	6	1.2	5.16×10^{-6}	129.2	8k	0	22.7	21.1
w6-32k-m129-a1.2	6	1.2	5.16×10^{-6}	129.2	32k	0	41.5	40.1
w6-8k-m517-a1.2	6	1.2	1.23×10^{-8}	516.6	8k	0	-	8.38
w6-32k-m517-a1.2	6	1.2	1.23×10^{-8}	516.6	32k	0	-	11.6

50 for $W_0 = 6$, which are consistent with previous results (Gürkan et al. 2004, and references therein). With a mass function, $t_{\rm cc}/t_{\rm rc}$ decreases as we increase $m_{\rm max}/\langle m\rangle$, and it follows $(m_{\rm max}/\langle m\rangle)^{-1}$ (dashed line in Figure 5) as far as $m_{\rm max}/\langle m\rangle \lesssim 30$.

We analytically derive the core-collapse time for models with stellar mass functions using the dynamical friction timescale of the most massive stars in the cluster, assuming that star clusters collapse when the most massive stars reach the cluster centre. The dynamical friction timescale of the most massive star with $m_{\rm max}$ is estimated from a simple equation. We follow the description in Binney & Tremaine (2008) in section 8.1.1., in which the dynamical friction timescale of a black hole which spirals in to the galactic centre is derived. We assume that the massive star has initially a circular orbit with velocity, $v_{\rm c}$, at a distance r from the cluster centre. From equation (8.9) in Binney & Tremaine (2008), the frictional force $F = m_{\rm max}|dv_m/dt|$ on the massive star is

$$F = \frac{4\pi G^2 m_{\rm max}^2 \rho(r) \ln\Lambda'}{v_{\rm c}^2}\left[{\rm erf}(X) - \frac{2X}{\sqrt{\pi}}\exp(-X^2)\right], \qquad (5)$$

where $X \equiv v_{\rm c}/(\sqrt{2}\sigma_{\rm 3D}) = 1$, where $\sigma_{\rm 3D}$ is the three-dimensional velocity dispersion and $v_{\rm c}$ is equivalent to the two-dimensional velocity dispersion. The value of the Coulomb logarithm here is different from that in equation (1), and therefore we describe it as $\ln\Lambda'$ (see Spinnato et al. (2003)). In order to simplify this equation, we assume the density distribution to be a singular isothermal sphere, $\rho(r) = v_{\rm c}^2/(4\pi G r^2)$, and then equation (5) becomes

$$F = 0.428 \ln\Lambda' \frac{G m_{\rm max}^2}{r^2}. \qquad (6)$$

The angular momentum change of the massive star due to the friction is

$$\begin{aligned} \frac{dL}{dt} &= -Fr \qquad (7)\\ &\simeq 0.428 \ln\Lambda' \frac{G m_{\rm max}^2}{r}. \qquad (8)\end{aligned}$$

In an isothermal sphere the circular velocity is independent of radius, and the angular momentum at radius r is written as $L = m_{\rm max} r v_{\rm c}$. With equation (8), we obtain

$$r\frac{dr}{dt} = -0.428 \frac{G m_{\rm max}}{v_{\rm c}}. \qquad (9)$$

The dynamical friction timescale of the most massive star is

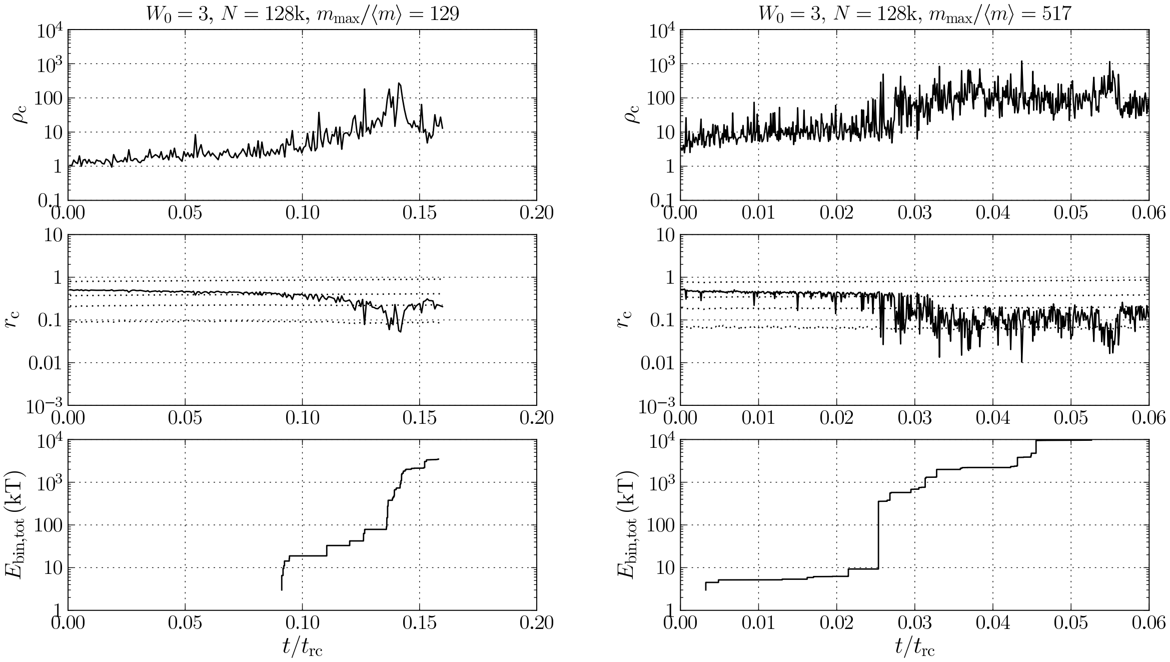

Figure 3. Same as Figure 1, but for models with N =128k and with $m_{\rm max}/(\langle m\rangle = 129$ (left) and 517 (right).

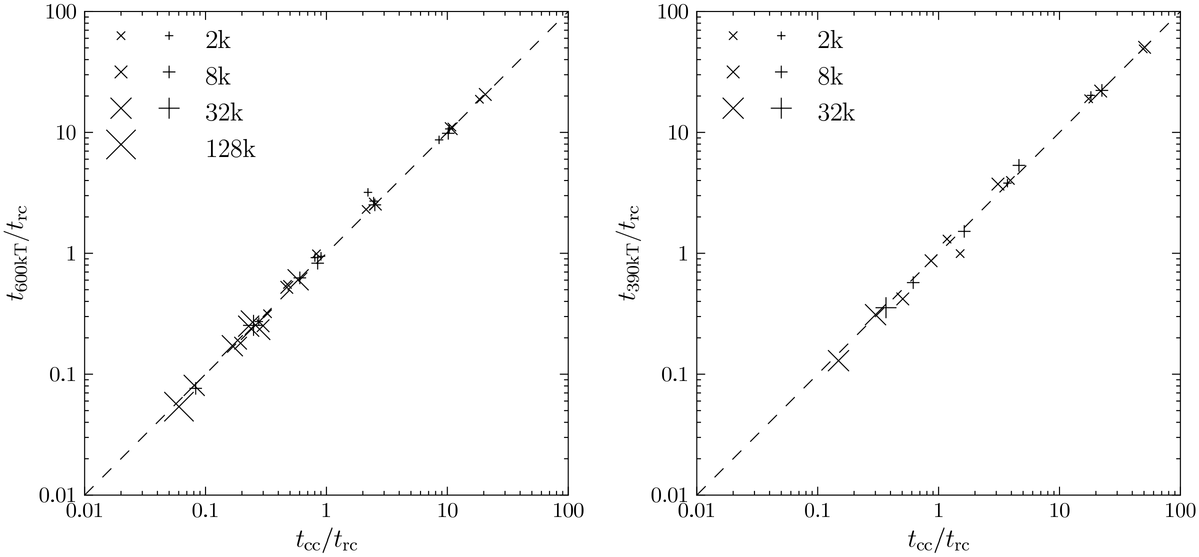

Figure 4. Comparison of two independent measurements of the moment of core collapse. Left panel: core-collapse time measured by the core density and core radius compared with the time of formation of $600kT$ binaries for $W_0 = 3$ (left panel) and for the formation of $390kT$ binaries for $W_0 = 6$ (right panel). The crosses indicate models with $\alpha = 2.35$, the plus-signs are for all other models.

finally written as

$$t_{\rm df} = \frac{1.65}{\ln \Lambda'} \frac{r^2 \sigma_{\rm 3D}}{G m_{\rm max}}. \qquad (10)$$

This result is shown in Figure 5 (dashed curves) and it is consistent with the simulations. Here, we adopted r as the half-mass radius and $\Lambda' = 0.1N$ (Giersz & Heggie 1994a; Heggie & Hut 2003). For the Coulomb logarithm for $t_{\rm rc}$, we adopted $\Lambda' = 0.1N_{\rm c}$, where $N_{\rm c} \equiv M_{\rm c}N$ is the number of particles in the core. The dynamical friction timescale of the most massive star is proportional to $m_{\rm max}^{-1}$, and as a consequence the core-relaxation time is proportional to

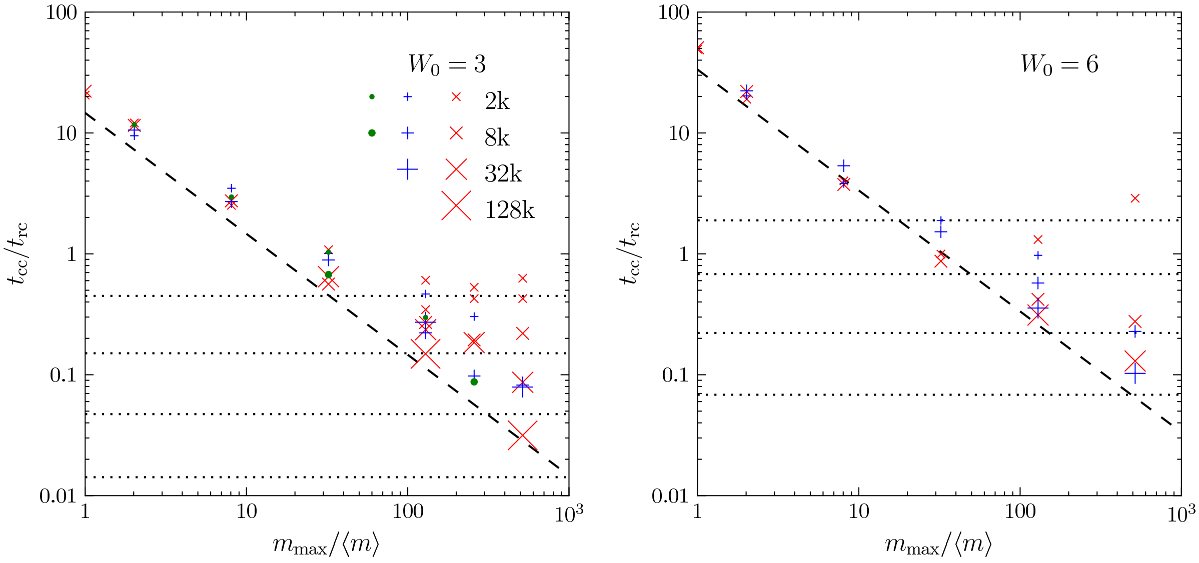

Figure 5. The core-collapse time as a function of the maximum mass of cluster particles, $m_{\rm max}/\langle m\rangle$ for models with $W_0 = 3$ (left panel) and 6 (right panel). Crosses, dots, and pluses indicate models with $\alpha = 2.35$ (Salpeter), 1.7, and 1.2, respectively. The sizes of the symbols indicate the number of particles. Dashed line shows the analytic results obtained from equation (10). The dotted lines indicate the minimum core-collapse time obtained from $10t_{\rm cross}$. They are for N = 2k, 8k, 32k, and 128k from top to bottom.

$\langle m\rangle^{-1}$ (see Eq. 1), and therefore we obtain that $t_{\rm cc}/t_{\rm rc} \propto (m_{\rm max}/\langle m\rangle)^{-1}$.

3.4 The minimum core-collapse time

As we see in Figure 5, models with fewer particles (N = 2k) deviate from the analytic result when $m_{\rm max}/\langle m\rangle \sim 30$. The critical value of $m_{\rm max}/\langle m\rangle$, however, depends on N. For models with N = 128k the simulations and theory give consistent results until $m_{\rm max}/\langle m\rangle \sim 500$. The models with N between 2k and 128k show a consistent picture of the moment that the models deviate from the theory for an increasing value of $m_{\rm max}/\langle m\rangle$ with respect to N. We bolster our earlier conclusion that a core bounce requires that $M/m_{\rm max} \gtrsim 100$. The core-collapse time saturates at smaller $m_{\rm max}/\langle m\rangle$ for models with fewer particles. We will discuss this critical value of $M/m_{\rm max}$ in section 4.1 and we will now focus to estimating the "minimum" core-collapse time we observe in Figure 5.

The minimum to the core-collapse time depends on N, which is a result of the dependency of $t_{\rm rc}$ on N. We consider that this minimum core-collapse time depends on the crossing time, $t_{\rm cross}$, of the cluster, because the dynamical friction time cannot be shorter than the crossing time. We adopt $t_{\rm cross} = \langle r^2\rangle^{1/2}/\sigma_{\rm 1D}$, where $\langle r^2\rangle^{1/2}$ is the root mean square of the distance from the cluster centre. The minimum core-collapse time obtained from the simulations is roughly consistent with $10t_{\rm cross}$. The dotted lines in Figure 5 give $10t_{\rm cross}$. Those lines also depend on N, because $t_{\rm cross}$ does not depend on N, whereas $t_{\rm rc}$ does.

4 DISCUSSION

4.1 N-dependence and comparison with single-component models

We discuss the criterion for an objective core collapse in the cases where $M/m_{\rm max} \gtrsim 10^3$ and for rapid core expansion in the case that $M/m_{\rm max} \gtrsim 100$. Here we will make an analogy with single-component models. From a wide range of analytic calculations and simulations, it is well established that the dynamical evolution of star clusters such as relaxation, core collapse, core bounce, and gravothermal oscillation depends on the total number of particles in the system (and in the core). For example, gravothermal oscillation occurs only when the number of particles exceed $\sim 10^4$ (Goodman 1987; Makino 1996). This criterion comes from the number of particles in the core after core bounce, $N_{\rm c}$. (Here we define $N_{\rm c}$ as the averaged number of particles after core collapse, and we adopt $N_{\rm cb}$ as the number of particles at the moment of core bounce.) The gravothermal oscillation occurs only when $N_{\rm c} > N_{\rm cb}$. While the value of $N_{\rm cb}$ is considered a constant in the range of 10 to 80 (Goodman 1987; Makino 1996; Hut 1996), $N_{\rm c}$ depends on N. If we adopt $N_{\rm c} \simeq N^{1/2}$ (Makino 1996), we can confirm that $N > 10^4$ satisfies $N_{\rm c} > N_{\rm cb}$.

The behaviour after core collapse changes when N decreases. So long as $N_{\rm c} \simeq N_{\rm cb}$ (i.e., $10^3 \lesssim N \lesssim 10^4$) we observe similar evolution but the collapse becomes shallower for smaller N, and the gravothermal oscillations disappear (see Fig. 1 in Makino 1996). For $100 \lesssim N \lesssim 10^3$ the core bounce disappears (see Figure 10 in Giersz & Heggie 1994b). These transitions are quite similar to those we observe if we increase $m_{\rm max}$. Our results of the multi-mass case are scalable to those of the single mass case if we define an effective number of particles ($N_{\rm eff}$) in the latter. For an equal mass system, $N_{\rm eff} \equiv N$, but when we introduce a spectrum

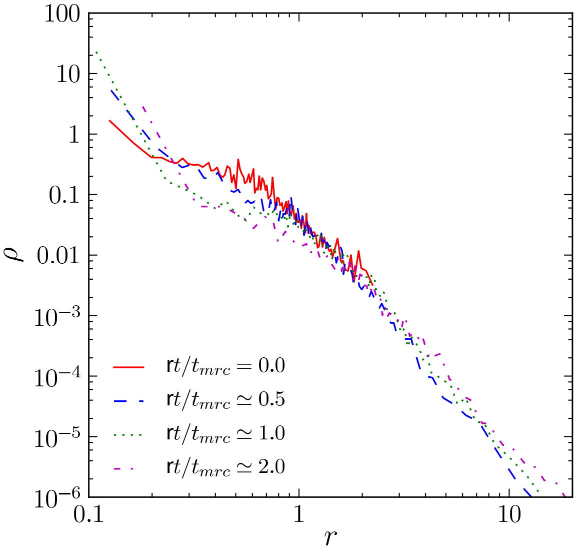

Figure 6. The evolution of the density profile for model w3-2k-m129-Sal-2 (the same model in the right panel of Figure 2).

of masses, $N_{\mathrm{eff}} = M/m_{\mathrm{max}}$. Interestingly, a similar conclusion is obtained from recent results for two-component and multi-component systems (Breen & Heggie 2012b,a).

If the number of particles drops below ~ 100, the behaviour of the N-body system changes from being a *many-body* system to a *few-body* system, which evolves chaotically (McMillan et al. 1988) rather than deterministic. In few-body systems it is hard to notice any core collapse in the evolution of core density and radius. In these cases the binary cannot harden to $\gtrsim 100kT$ because the total energy budget of the cluster $\lesssim 100kT$. In such systems the hard binary stops interacting with other cluster members when it becomes too tight and the surrounding density becomes too low. As a result, the "tenured" or "frozen binary" remains in the cluster (Casertano 1985). This situation is seen in multi-mass model if $M/m_{\mathrm{max}} \lesssim 100$ (see Figure 2). The dynamical evolution of frozen binaries almost stops in this case, but the frozen binary is still in the cluster, and likely to be in the core. In Figure 6 we present the evolution of density profiles of model w3-2k-m129-Sal-2 (we used the same model in the right panel of Figure 2). The frozen binary and its relatively low-density environment are noticeable as the high density peak in the centre and a depletion in the more extended core. This effect is similar to the core mass-deficiency arguments used in the nuclei with binary black holes after a major galaxy merger (Merritt 2010). In the formation process of frozen binaries, massive particles concentrated in the cluster centre are ejected from the cluster by sling-shot interactions with the binary. This mechanism leads to the formation of massive runaway stars around dense, young star clusters (Fujii & Portegies Zwart 2011).

4.2 Dynamical evolution driven by the most massive stars

The dynamical evolution of equal-mass models scales with t_{rc} irrespective of the particle number (Spitzer 1987). We confirm this hypothesis with our multi-mass simulations, so long as $M/m_{\mathrm{max}} \gtrsim 100$. For multi-mass models, however, $t_{\mathrm{cc}}/t_{\mathrm{rc}}$ decreases for increasing $m_{\mathrm{max}}/\langle m\rangle (\equiv f_{\mathrm{max}})$, and we demonstrate that t_{cc} is determined by the dynamical friction timescale of the most massive stars in the cluster. Here we show that the dynamical evolution of star clusters with a mass function is driven by the most massive stars in the cluster.

The relaxation time of a multi-mass system is dominated by the dynamics of the most massive star, and the global relaxation time is a factor of $F_{\mathrm{m}} \equiv \ln(\gamma N/f_{\mathrm{max}})/(f_{\mathrm{max}} \ln(\gamma N))$ shorter than that of an equal mass system. In Figure 7, we present the evolution of the core density scaled in time by the product of t_{rc} and F_{m}. As long as the model satisfies the condition of core collapse ($M/m_{\mathrm{max}} \gtrsim 10^3$), the evolutionary tracks of the core density are scaled with $F_{\mathrm{m}} t_{\mathrm{rc}}$. The scaling parameters are determined using the initial cluster. When the cluster approaches core collapse, the models with a mass function start to deviate from the equal-mass case.

The maximum core density, $\rho_{\mathrm{c,max}}$, reached the moment of the core collapse (the depth of the core collapse) decreases as $m_{\mathrm{max}}/\langle m\rangle$ increases. We present the relation between $\rho_{\mathrm{c,max}}$ and $m_{\mathrm{max}}/\langle m\rangle$ in Figure 8. This phenomenon is similar to the relation between the maximum density and N (Giersz & Heggie 1994b). If we try to understand this following the discussion in Hut (1996), in which it is derived that $\rho \propto N^{-2}$, we expect that the maximum density decreases following $(m_{\mathrm{max}}/\langle m\rangle)^{-2}$ assuming that the core consists of the most massive stars and therefore that $\rho \propto N_{\mathrm{eff}}^{-2}$. In Figure 8, however, the power is shallower than -2, although we see the trend that the maximum density decreases for increasing $m_{\mathrm{max}}/\langle m\rangle$. This might be because the mean particle mass in the core is smaller than m_{max}. Note that we can measure the core density only in a snapshot, which is limited by our output frequency. We therefore are likely to miss the highest density peak; it is very difficult to catch the exact moment of the highest density in an N-body simulations. This can be solved by storing the particle position and velocity information in a time resolved data format, as was proposed in Faber et al. (2010) (see also Farr et al. (2012)).

4.3 Comparison with previous results

We find that $t_{\mathrm{cc}}/t_{\mathrm{rc}} \propto (m_{\mathrm{max}}/\langle m\rangle)^{-1}$, which is inconsistent with a previous work by Gürkan et al. (2004), who conclude that the core-collapse time is proportional to $(m_{\mathrm{max}}/\langle m\rangle)^{-1.3}$. This discrepancy can be attributed to their use of a Monte-Carlo code, which cannot properly follow the cluster all the way to the moment of core collapse, but shows core bounce at some earlier instance. A hint of the early termination of their calculations is visible in their Fig. 2, where the Lagrangian radii of the simulations with a mass function suddenly truncates. They identify this moment as core collapse, but by inspection of our own simulations the sudden break in the inner most Lagrangian radii is generally associated with the formation of the first hard (few kT)

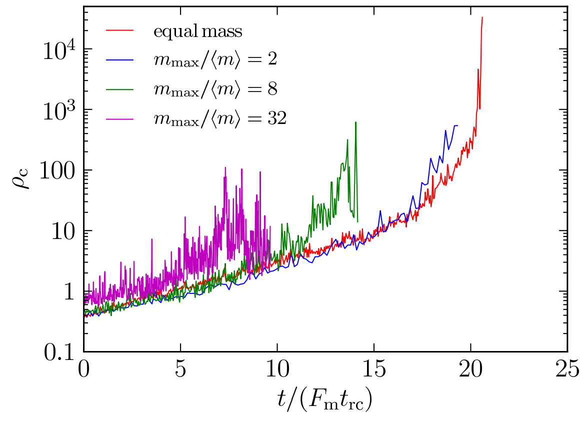

Figure 7. Evolution of the core density scaled by $t_{\rm rc}$ and the factor of the relaxation time for the most massive stars, $F_{\rm m}$, for models with $N = 8$k, $W_0 = 3$, and $\alpha = 2.35$.

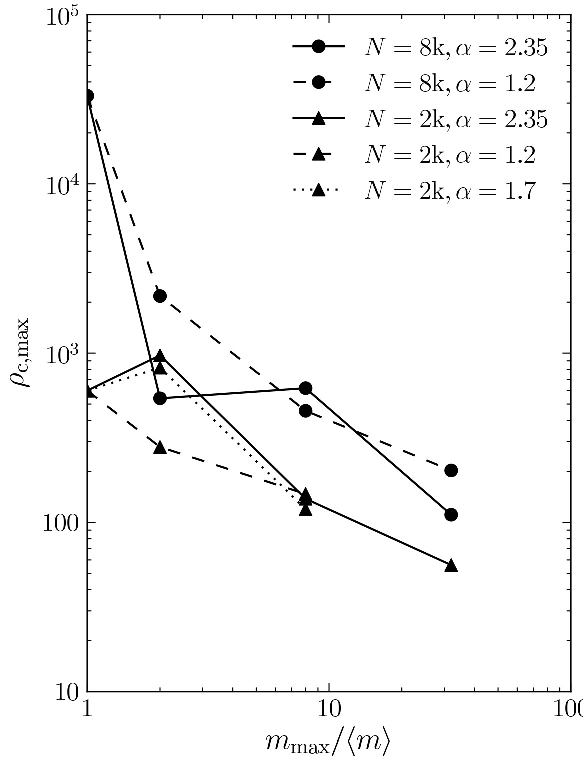

Figure 8. The maximum density reached during core collapse as a function of the mass of the most massive star in terms of the mean mass $m_{\rm max}/\langle m\rangle$.

binary. We tested this hypothesis by analysing the results of our simulation up to the moment of the formation of the first hard ($3kT$) binary. In figure 9, we present the formation time of the first $3kT$-binary, t_{3kT}, for models with $W_0 = 3$ as a function of $m_{\rm max}/\langle m\rangle$. With our adopted formation of the first hard binary our results become consistent with those of Gürkan et al. (2004), and we argue that $t_{3kT}/t_{\rm rc} \propto (m_{\rm max}/\langle m\rangle)^{-1.3}$ and saturates at $t_{\rm cc}/t_{\rm rc} = 0.15$.

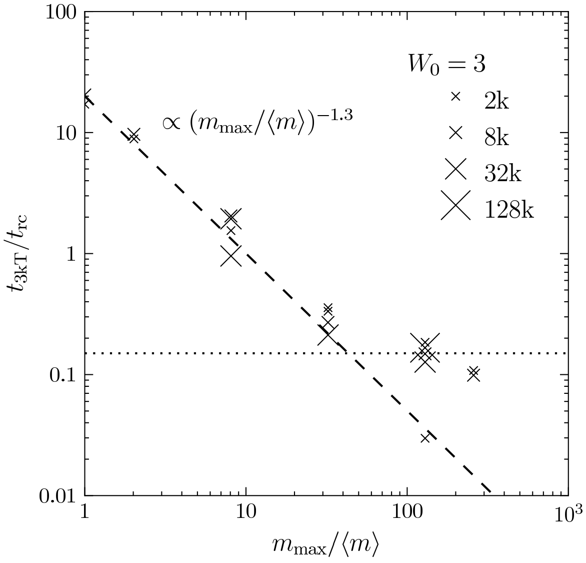

Figure 9. The moment of the formation of the first 3kT binary (the hard binary limit according to Tanikawa & Fukushige 2009) as a function of the maximum mass of the cluster particles, $m_{\rm max}/\langle m\rangle$ for $W_0 = 3$ and Salpeter MF models. Models with $m_{\rm max}/\langle m\rangle = 517$ initially host 3kT binaries, and therefore they are not plotted in this figure. Dashed line shows $20 \times (m_{\rm max}/\langle m\rangle)^{-1.3}$. The dotted lines indicate the $t_{\rm 3kT}/t_{\rm rc} = 0.15$, which is suggested the minimum ratio between $t_{\rm cc}$ and $t_{\rm rc}$ by Gürkan et al. (2004).

5 CONCLUSIONS

We performed a series of N-body simulations of star clusters with various mass ranges and power laws of the mass function, and found that the core-collapse time follows $t_{\rm cc}/t_{\rm rc} \propto (m_{\rm max}/\langle m\rangle)^{-1}$ for clusters with $M/m_{\rm max} \gtrsim 100$. When $M/m_{\rm max} \lesssim 100$, this relation breaks and $t_{\rm cc}$ saturates at $\sim 10t_{\rm cross}$. Using analytic arguments we derived that star clusters with a mass function reach core collapse in the dynamical friction timescale of the most massive stars. We also showed that the dynamical evolution of star clusters with a mass function are driven by the relaxation timescale of the most massive stars. We define an effective number of stars $N_{\rm eff} = M/m_{\rm max}$ for which a multi-mass cluster shows a similar core collapse behaviour as in the equal-mass case.

When the mass of the most massive stars is relatively small ($M/m_{\rm max} \gtrsim 10^3$), we notice a pronounced peak in the core density during the evolution. As we increase the mass of the most massive stars, $m_{\rm max}$, the peak at the core bounce becomes lower. We found that the binding energy of the hard binaries are a good indicator for detecting the moment of the core collapse, even if the density peak is ambiguous. We adopted that the critical binding energy of hard binaries, with which the binary emits sufficient energy to bounce the core and eject stars from the system, as the moment of the core bounce. We conclude that the binding energy criterion gives a more robust indicator for the core-collapse time compared to inspection of the core density and radius.

ACKNOWLEDGMENTS

We thank Jeroen Bédorf for discussions and adapting the Sapporo2 library to sixth order and Alex Rimoldi for careful reading of the manuscript. This work was supported by Postdoctoral Fellowship for Research Abroad of the Japan Society for the Promotion of Science (JSPS) and by Netherlands Research Council NWO (#639.073.803 [VICI] and #614.061.608 [AMUSE]). Numerical computations were carried out on Cray XT-4 CPU-cluster at the Center for Computational Astrophysics (CfCA) of the National Astronomical Observatory of Japan and the Little Green Machine at Leiden Observatory (NWO grant #612.071.305).

REFERENCES

Aarseth S. J., 1974, A&A, 35, 237

Bédorf J., Portegies Zwart S., 2012, European Physical Journal Special Topics, 210, 201

Belleman R. G., Bédorf J., Portegies Zwart S. F., 2008, New A, 13, 103

Bettwieser E., Sugimoto D., 1984, MNRAS, 208, 493

—, 1985, MNRAS, 212, 189

Binney J., Tremaine S., 2008, Galactic Dynamics: Second Edition. Princeton University Press

Breen P. G., Heggie D. C., 2012a, MNRAS, 425, 2493

—, 2012b, MNRAS, 420, 309

Casertano S., 1985, in IAU Symposium, Vol. 113, Dynamics of Star Clusters, Goodman J., Hut P., eds., pp. 305–308

Casertano S., Hut P., 1985, ApJ, 298, 80

Cohn H., 1979, ApJ, 234, 1036

—, 1980, ApJ, 242, 765

Faber N. T., Stibbe D., Portegies Zwart S., McMillan S. L. W., Boily C. M., 2010, MNRAS, 401, 1898

Farr W. M., Ames J., Hut P., Makino J., McMillan S., Muranushi T., Nakamura K., Nitadori K., Portegies Zwart S., 2012, New A, 17, 520

Fujii M. S., Portegies Zwart S., 2011, Science, 334, 1380

Giersz M., Heggie D. C., 1994a, MNRAS, 268, 257

—, 1994b, MNRAS, 270, 298

—, 1996, MNRAS, 279, 1037

Goodman J., 1987, ApJ, 313, 576

Goswami S., Umbreit S., Bierbaum M., Rasio F. A., 2012, ApJ, 752, 43

Gürkan M. A., Freitag M., Rasio F. A., 2004, ApJ, 604, 632

Heggie D., Hut P., 2003, The Gravitational Million-Body Problem: A Multidisciplinary Approach to Star Cluster Dynamics, Heggie D. & Hut P., ed.

Heggie D. C., 1975, MNRAS, 173, 729

Hut P., 1983, ApJ, 272, L29

—, 1996, in IAU Symposium, Vol. 174, Dynamical Evolution of Star Clusters: Confrontation of Theory and Observations, Hut P., Makino J., eds., p. 121

Inagaki S., 1980, PASJ, 32, 213

Inagaki S., Wiyanto P., 1984, PASJ, 36, 391

King I. R., 1966, AJ, 71, 64

Lynden-Bell D., Eggleton P. P., 1980, MNRAS, 191, 483

Lynden-Bell D., Wood R., 1968, MNRAS, 138, 495

Makino J., 1996, ApJ, 471, 796

Makino J., Tanekusa J., Sugimoto D., 1986, PASJ, 38, 865

McMillan S., Casertano S., Hut P., 1988, in Astrophysics and Space Science Library, Vol. 140, IAU Colloq. 96: The Few Body Problem, Valtonen M. J., ed., pp. 313–317

Merritt D., 2010, ApJ, 718, 739

Nakada Y., 1978, PASJ, 30, 57

Nitadori K., Makino J., 2008, New Astronomy, 13, 498

Nitadori K., Makino J., Abe G., 2006, ArXiv Astrophysics e-prints

Portegies Zwart S. F., McMillan S. L. W., 2002, ApJ, 576, 899

Salpeter E. E., 1955, ApJ, 121, 161

Spinnato P. F., Fellhauer M., Portegies Zwart S. F., 2003, MNRAS, 344, 22

Spitzer L., 1987, Dynamical evolution of globular clusters

Spitzer Jr. L., Hart M. H., 1971, ApJ, 164, 399

Spitzer Jr. L., Shull J. M., 1975, ApJ, 200, 339

Sugimoto D., Bettwieser E., 1983, MNRAS, 204, 19P

Takahashi K., 1995, PASJ, 47, 561

Tanikawa A., Fukushige T., 2009, PASJ, 61, 721